Supplementary Information for

Exocytosis at the hair cell ribbon synapse apparently operates without neuronal SNARE proteins

Régis Nouvian, Jakob Neef, Anna V. Bulankina, Ellen Reisinger, Tina Pangršič, Thomas Frank, Stefan Sikorra, Nils Brose, Thomas Binz and Tobias Moser

Nature Neuroscience: doi:10.1038/nn.2774

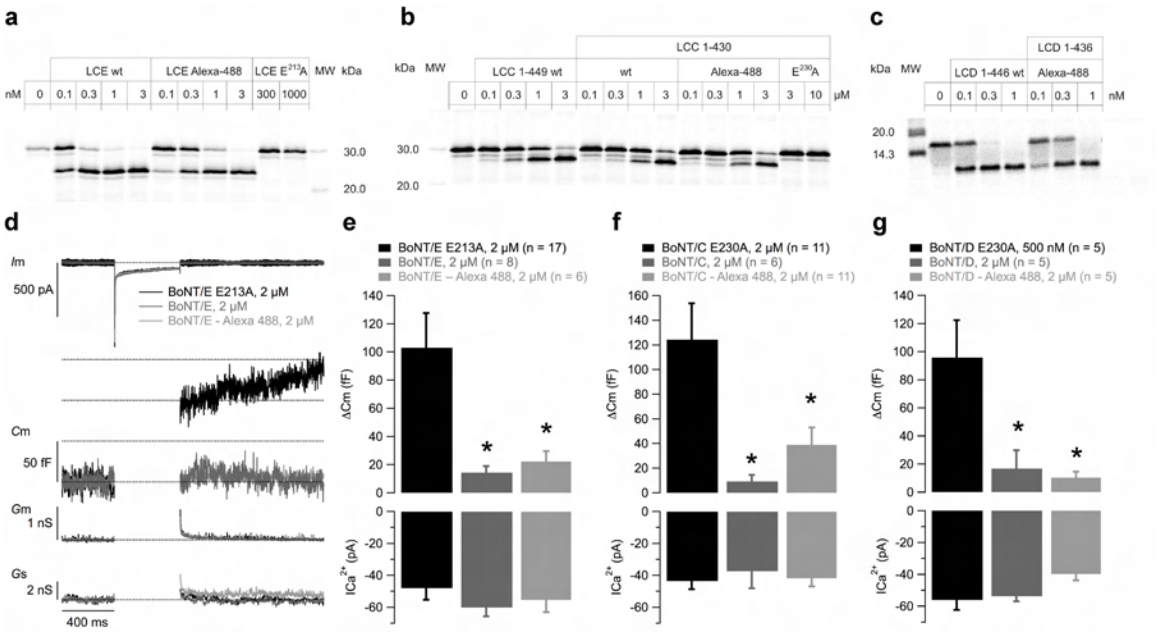

Supplementary Fig. 1: Biochemical and functional activity of BoNT light chains.

(**a**–**c**) *In vitro* cleavage activity of BoNT light chains. (**a**) Cleavage of ^{35}S-SNAP-25-His$_6$ by unlabeled full-length or by Alexa488-labeled BoNT/E light chain, no cleavage by the inactive E213A mutant BoNT/E light chain. (**b**) Cleavage of ^{35}S-SNAP-25-His$_6$ by unlabeled full-length or Alexa488-labeled shortened BoNT/C light chain, no cleavage by the inactive E230A mutant BoNT/C light chain. (**c**) Cleavage of ^{35}S-synaptobrevin-2 by unlabeled full-length BoNT/D or Alexa488-labeled shortened light chain. (**d-g**) Efficient block of chromaffin cell exocytosis by BoNT light chains. (**d**) Representative membrane current (I_m), membrane capacitance (C_m), membrane conductance (G_m) and series conductance (G_s) traces (from top to bottom) elicited by 500 ms step depolarization to –27 mV from a holding potential of –87 mV. Data were recorded from mouse chromaffin cells after infusing for 10 min with the inactive (black), active (dark grey) and Alexa488-conjugated (light grey) BoNT/E light chain. (**e**–**g**) Summed capacitance responses after 10 min of infusion with the inactive (black), active (dark grey) and Alexa488-conjugated (light grey) BoNT/E (**e**), BoNT/C (**f**) and BoNT/D (**g**) light chain. Data represent mean ± s.e.m. (*p<0.05, Mann-Whitney test). Summed Ca^{2+} current amplitude (bottom) was measured between 100 and 400 ms of the depolarization (after Na^+ current inactivation).

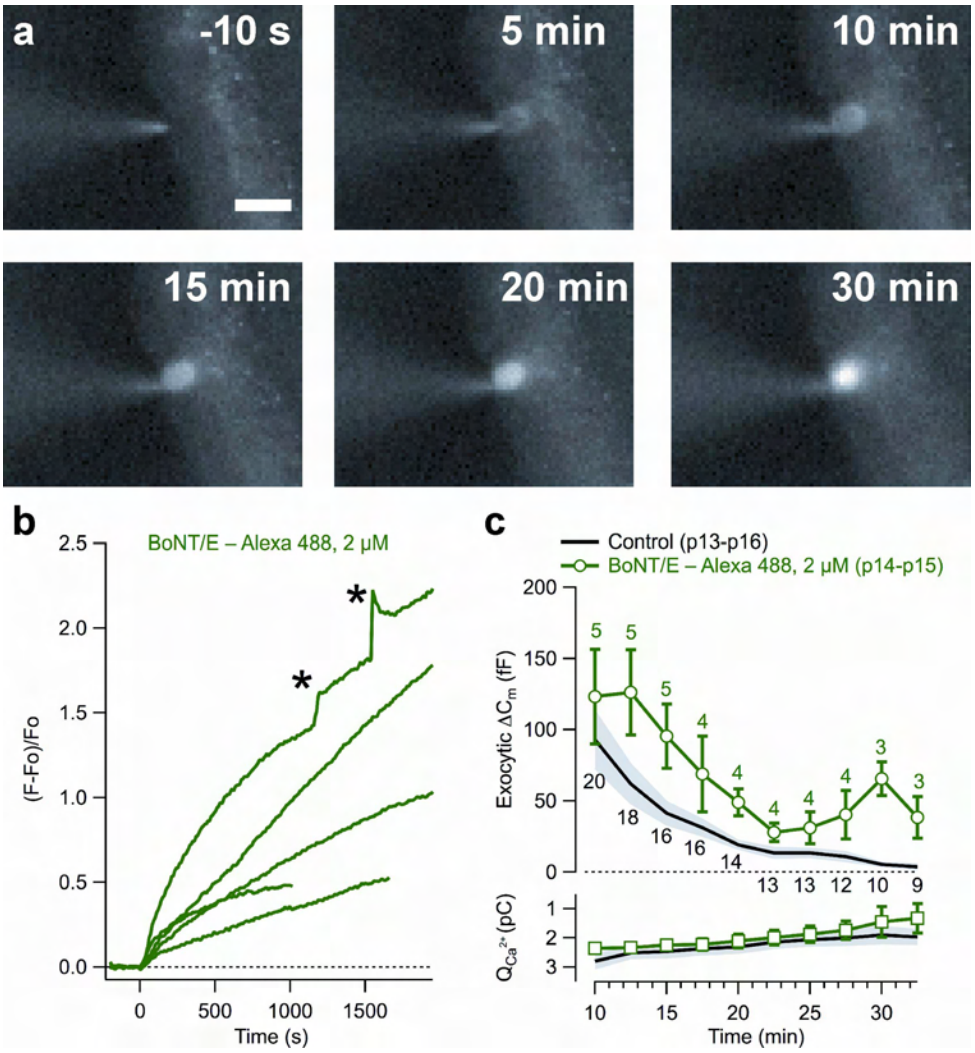

Supplementary Fig. 2: Diffusion of Alexa488-conjugated BoNT/E into IHC somata.

(**a**) Fluorescent images at 480 nm excitation of an IHC filled via the patch-pipette with Alexa488-conjugated BoNT/E dye. Time indicated in the panels is relative to the plasma membrane break-in in order to establish whole cell configuration. Scale bar: 20 µm. (**b**) Time course of the Alexa488-conjugated BoNT/E fluorescence in IHCs. The sudden increases of fluorescence indicated by asterisks reflect applications of positive pressure to the patch-pipette. (**c**) Average exocytic ΔCm and calcium current integral (Q_{Ca}^{2+}) plotted against each 20 ms step depolarization trial. Numbers in (**c**) indicate IHC counts for each trial.

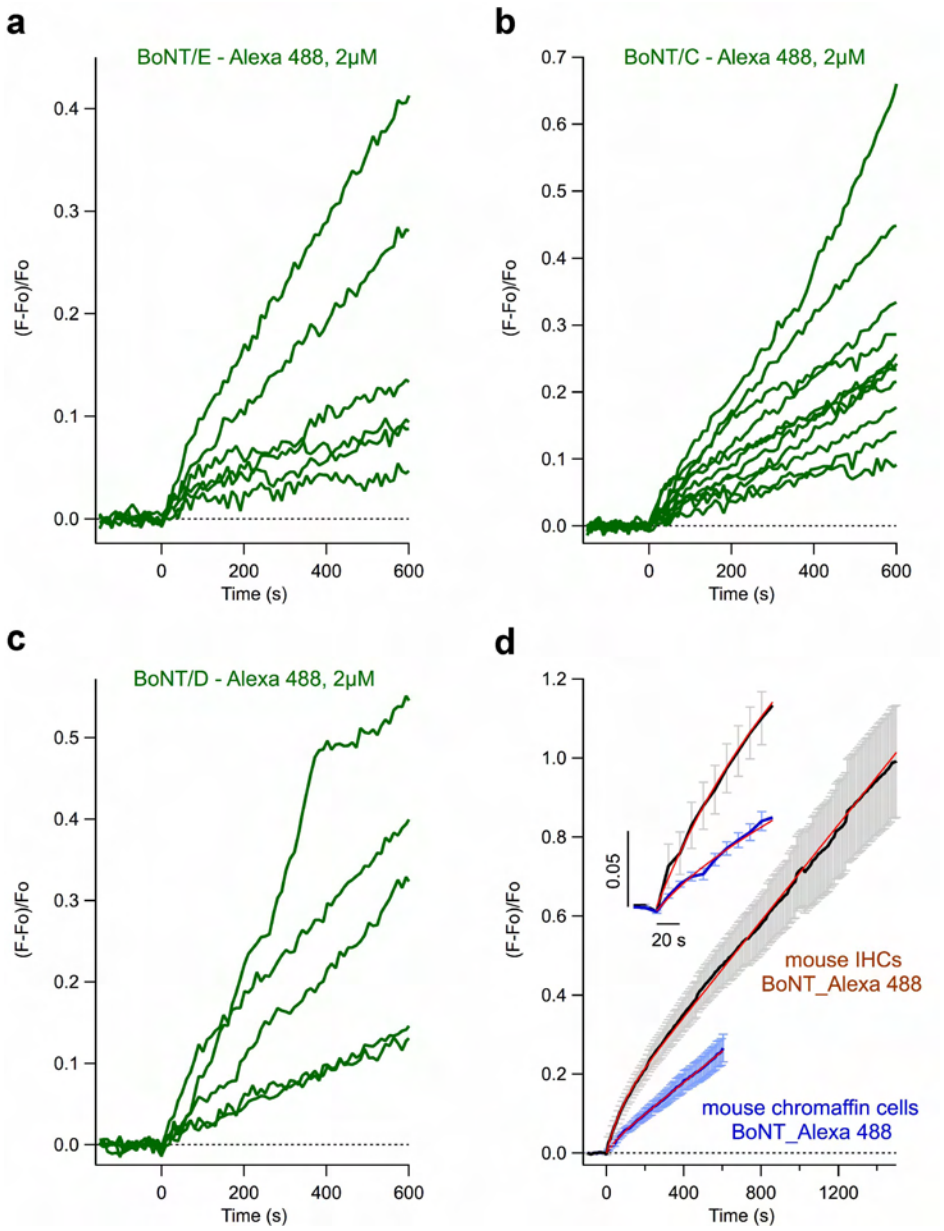

Supplementary Fig. 3: Diffusion of Alexa488-conjugated BoNT into mouse chromaffin cells (a–d) and IHCs (d).

Time course of the Alexa488-conjugated BoNT/E (**a**), BoNT/C (**b**) and BoNT/D (**c**) fluorescence in mouse chromaffin cells. Time 0 represents the plasma membrane break-in in order to establish whole cell configuration. (**d**) Average time course of Alexa488-conjugated BoNT fluorescence in chromaffin cells (blue, n = 22) and inner hair cells (black, n = 23) overlaid with the sum of an exponential and a line fit (red). Inset: first 100 seconds of the fluorescence rise.

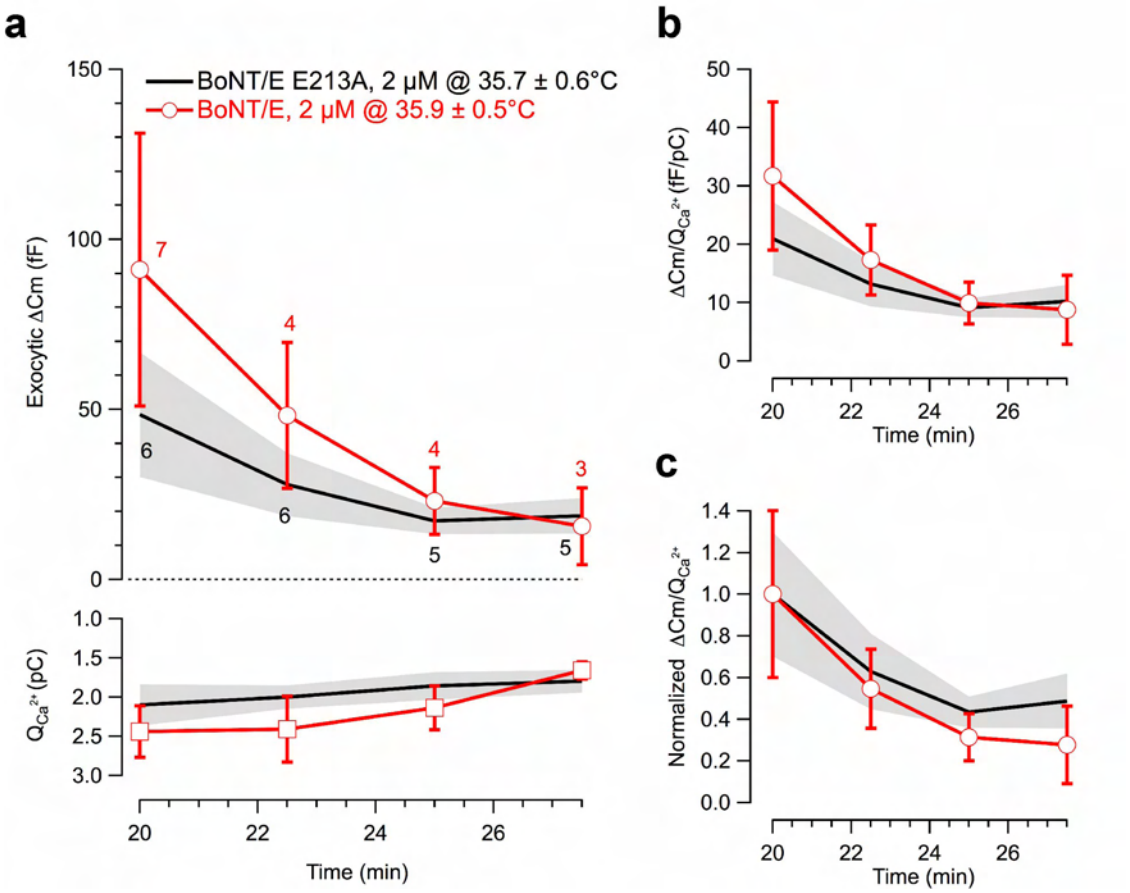

Supplementary Fig. 4: Exocytosis in inner hair cells resists BoNT/E attack at physiological temperature for more than 20 min.

(**a**) Average exocytic ΔC_m (upper panel) and calcium charge (Q_{Ca}^{2+}; lower panel), (**b**) exocytosis per unit of incoming Ca^{2+} ions ($\Delta C_m/Q_{Ca}^{2+}$) and (**c**) $\Delta C_m/Q_{Ca}^{2+}$ ratio normalized to the averaged first response plotted for each 20 ms step depolarization trial in BoNT/E light chain poisoned (red) and inactive toxin infused IHCs (black). Data were recorded from IHCs after 20-minute infusion with either the active BoNT/E light chain or with the inactive toxin at 35°C with successive 20 ms depolarizations to –27 mV from a holding potential of –87 mV. The number of recorded IHCs is indicated for each trial in (**a**).

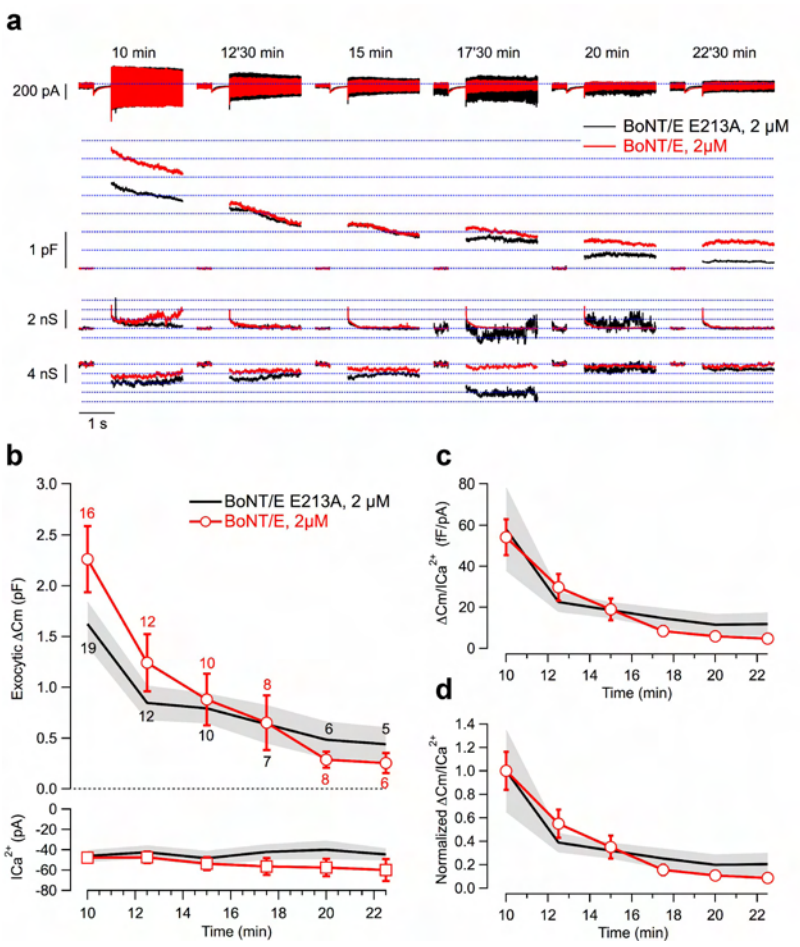

Supplementary Fig. 5: Exocytosis evoked by long depolarizations in IHCs is resistant to BoNT/E attack.

(**a**) Representative whole-cell patch-clamp Ca^{2+} current (I_{Ca}^{2+}), membrane capacitance (C_m), membrane conductance (G_m) and series conductance (G_s) traces (from top to bottom) elicited by successive 500 ms depolarizations to –27 mV from a holding potential of –87 mV. Data were recorded from IHCs after infusing with the active BoNT/E light chain (red) or with the inactive toxin (black) for 10 minutes. (**b**) Average exocytic ΔC_m (upper panel) and calcium current (I_{Ca}^{2+}; lower panel), (**c**) exocytosis per unit of incoming Ca^{2+} ions ($\Delta C_m/I_{Ca}^{2+}$) and (**d**) $\Delta C_m/I_{Ca}^{2+}$ ratio normalized to the averaged first response plotted against each 500 ms step depolarization trial in BoNT/E light chain poisoned IHCs (red) and IHCs infused with inactive toxin (black). IHC Ca^{2+} current amplitude was measured over the last 400 ms of the depolarization. The number of recorded IHCs is indicated for each trial in (**b**).

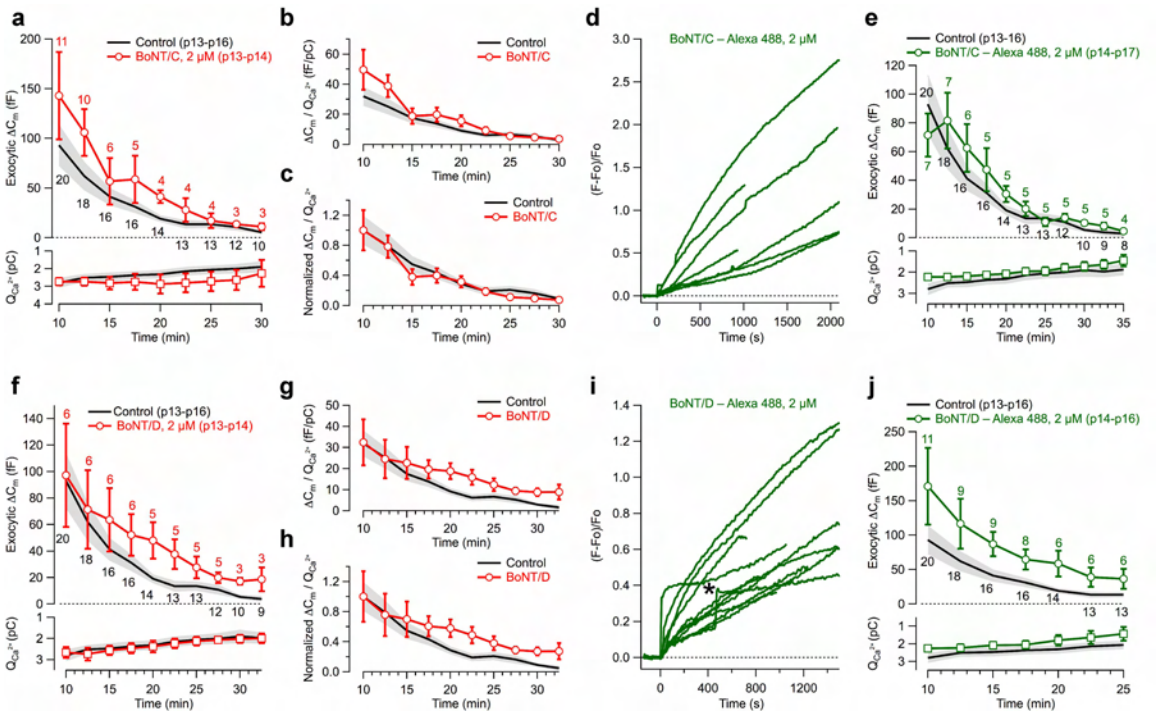

Supplementary Fig. 6: IHC exocytosis is resistant to BoNT/C and BoNT/D.

(**a, f**) Average exocytic ΔC_m and Ca^{2+} current integral (Q_{Ca}^{2+}) plotted against each 20 ms step depolarization trial. Data were recorded from IHCs after infusing for 10 min with the BoNT/C (**a**) or BoNT/D (**f**) light chain (red) or without toxins (control, black). The number of recorded IHCs is indicated for each trial. (**b**, **g**) Exocytosis per unit of incoming Ca^{2+} ions ($\Delta C_m/Q_{Ca}^{2+}$) and (**c**, **h**) $\Delta C_m/Q_{Ca}^{2+}$ ratio normalized to the first response from IHCs poisoned with BoNT/C (**b**, **c**) or BoNT/D (**g**, **h**) light chain (red) or without toxins (control, black). (**d**, **i**) Time course of the Alexa488-conjugated BoNT/C (**d**) and BoNT/D (**i**) fluorescence in IHCs (both green). 0 sec refers to the plasma membrane break-in in order to establish whole-cell configuration. The sudden increase of fluorescence indicated by an asterisk in (**i**) reflects application of positive pressure to the patch-pipette. (**e, j**) Average exocytic ΔC_m and Q_{Ca}^{2+} plotted against each 20 ms step depolarization trial for the corresponding experiment in (**d**) and (**i**).

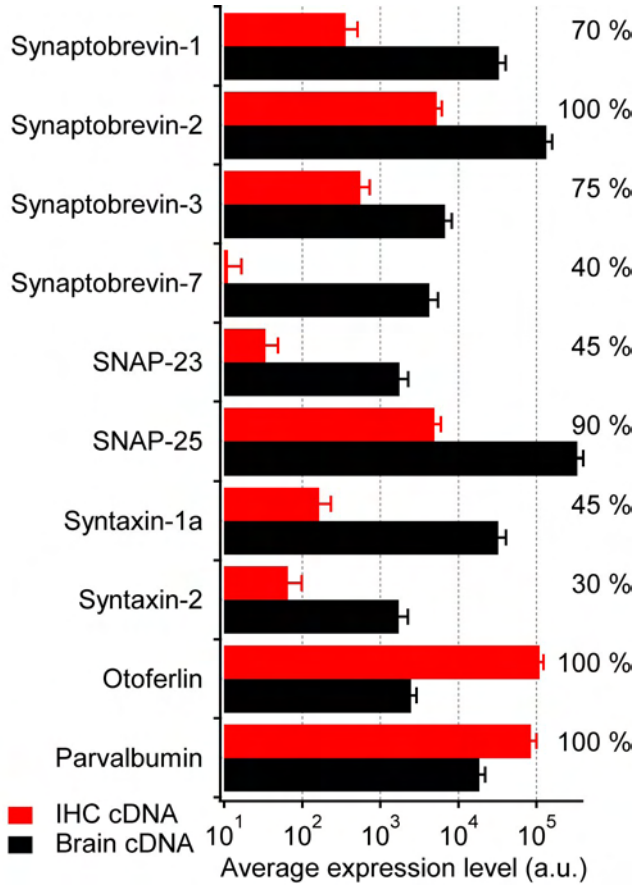

Supplementary Fig. 7: mRNA expression of SNARE proteins in IHCs.

Quantification of transcripts in 20 IHCs (red bars) by means of 15-cycle multiplex PCR followed by real-time PCR with taqman probes. Percentages indicate in how many of the 20 cells the transcript was found by a fluorescence increase in real-time PCR. Values in a.u. were calculated from the C_t values, which are the cycle numbers at which the fluorescence indicating amplification of the transcript reached threshold, as *Expression level* = 2^{42-Ct} (assuming that a single cDNA molecule would result in a C_t value of 42 - deviations from this assumption would result in a linear scaling of the a.u. given here). Brain cDNA (black bars) used as positive control was diluted 1000-fold and not pre-amplified by multiplex PCR.

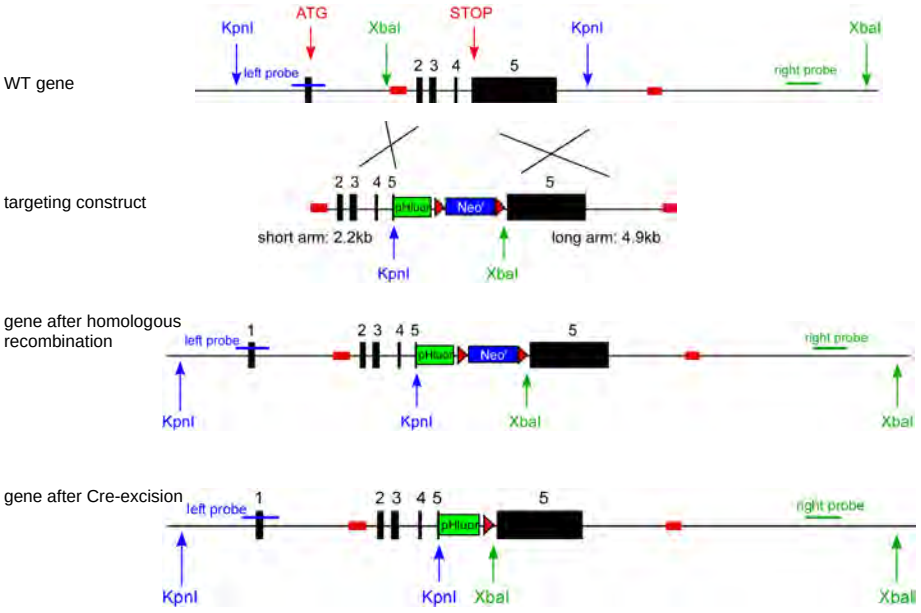

Supplementary Fig. 8: Knock-in of pHluorin into the synaptobrevin-1 locus by homologous recombination.

The original stop codon of the wild type synaptobrevin-1 was replaced by the cDNA encoding superecliptic pHluorin[1]. Downstream of the stop codon of pHluorin, a Neomycin selection cassette was introduced which was later excised by Cre recombination.

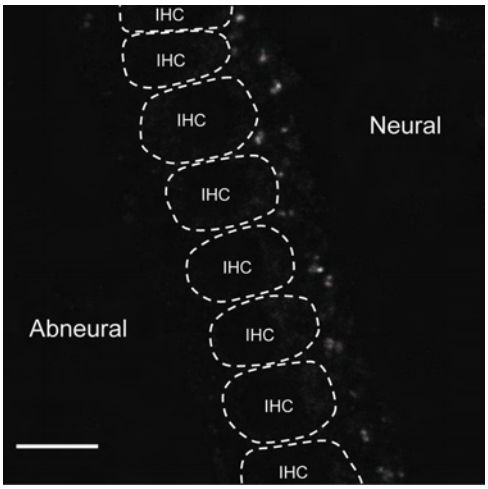

Supplementary Fig. 9: Localization of genetically labeled synaptobrevin-1.

Maximum-intensity projection of confocal slices of endogenous synaptopHluorin-fluorescence in acute organ of Corti explants did not reveal noticeable fluorescence in IHCs even upon dequenching of the pHluorin by application of NH_4Cl (as shown here). The fluorescent spots appeared to be located outside the IHCs, and no increase in fluorescence was observed upon depolarization of IHCs (whole-cell patch-clamp), indicating that these spots represent efferent synapses. Scale bar: 10 μm.

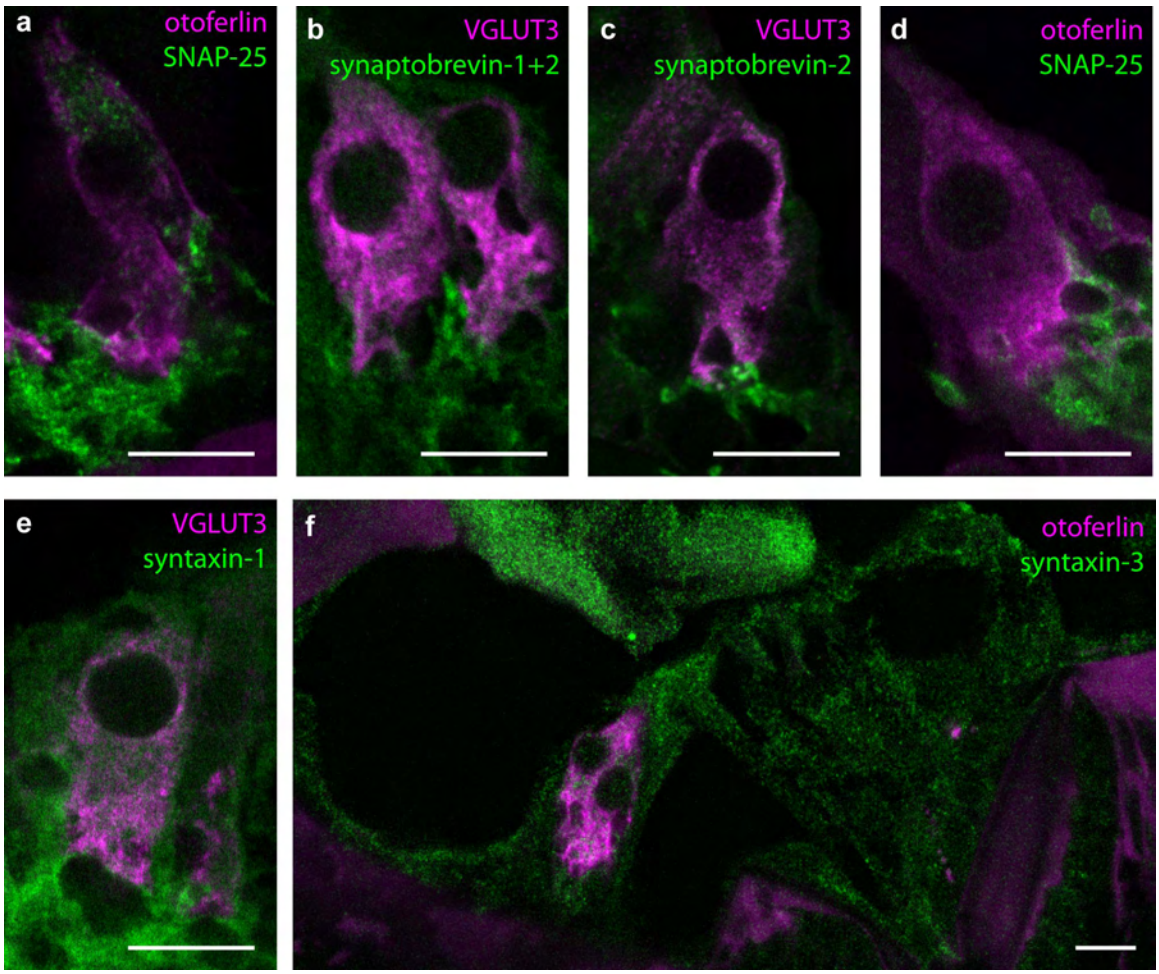

Supplementary Fig. 10: Immunohistochemistry for neuronal SNAREs.

(**a**–**e**) Hair cells were labeled with antibodies directed against otoferlin (**a**, **d**, **f**) or VGLUT3 (**b**–**c**, **e**) (both magenta) and the respective neuronal SNAREs (green). (**a**) The Abcam ab5666 anti-SNAP-25 antibody showed weak staining in the apical part of IHCs, but no labeling in the basolateral compartment. (**b**) No staining of the IHC was observed with the Stressgen VAM-SV014 anti-synaptobrevin-1+2 antibody. For (**c**–**e**) we applied the long-lasting fixation paradigm employed by Safieddine and Wenthold[2], who demonstrated IHC labeling for SNAREs in the guinea pig. Using the Synaptic Systems 104 211 (69.1) anti-synaptobrevin-2 (**c**), Abcam ab5666 anti-SNAP-25 (**d**) or Sigma s0664 anti-syntaxin-1 antibodies (**e**), we could not find consistent and specific labeling of mouse IHCs. (**f**) No specific staining was detected in the organ of Corti with the Synaptic Systems 110 032 anti-syntaxin-3 antibody. Scale bars: 10 µm.

	Inner hair cells	Mouse chromaffin cells
Volume (pl)	2.2 (ref. 3)	1.2 (ref. 4)
Average R_S (MΩ)	11.5	14.5
Time constant[5] (s)	300	200
Toxin concentration after 5 min (μM)	1.3	1.6
Toxin copies inside cell	1.7 Mio	1.2 Mio
Number of vesicles	200,000 - 600,000 (ref. 3)	22,000 (ref. 6)
Synaptobrevin copies[7]	14 - 42 Mio	1.5 Mio
Syb/BoNTD ratio	8 to 25	1.3

Supplementary Table 1: Calculation of time constants of toxin infusion into inner hair cells and chromaffin cells.

Time constants were calculated and corrected for volume as proposed by Pusch & Neher[5] as $\tau = 0.6 \times R_S \times M^{1/3} \times \frac{V}{V_0}$, where R_S is the series resistance in MΩ, M is the infused molecule's mass in Da (50,000 for BoNT/D-LC), V is the cell's volume in pl and V_0 is the average volume of Pusch & Neher's bovine chromaffin cells (1.897 pl). From these and the toxin concentration inside the patch pipette (2 μM), the theoretical toxin contents inside the cells after 5 minutes of infusion were calculated. The numbers of synaptobrevin copies inside the cell were calculated from the IHC synaptic vesicle and chromaffin cell granule number estimates multiplied by the synaptobrevin copies per vesicle (70; ref. 7).

Gene	ID	forward external primer (5'-3')	reverse external primer (5'-3')	Taqman assay (Applied Biosystems)
Synaptobrevin-1	NM_001080557	CGTCTCGTTGCATTCTCC	CCGCCTGTTACTGGTCATG	Mm00772307_m1
Synaptobrevin-2	NM_009497.3	AAACAAGTGCAGCCAAGCTC	GAGAGGCCCTTCTTAGGCAG	Mm01325243_m1
Synaptobrevin-3	NM_009498.4	GTGCCTCGCAGTTTGAAAC	GATCCTGAATATCGGGCTTC	Mm_VAMP3-3exo
Synaptobrevin-7	NM_011515.4	AAGGAATAATGGTCAGAAACATAGAT	GTGAGCTTGATATTCTTCATACACA	Mm_VAMP7-6exo
SNAP-23	NM_009222.3	CCAGCAGTGTGACGACTCA	TCATCCAGCATAGTGATGGTCT	Mm01330351_mH
SNAP-25	NM_011428.3	ACCATGGCCGAAGACG	CCTTGCTCATCCAACATAACC	Mm01336180_m1
Syntaxin-1a	NM_016801.3	GAGCACGCCGTGGACTAC	TGGTTTCTATCCAAAGATGCC	Mm01196307_m1
Syntaxin-2	NM_007941.2	TGTTCCGGGAGCGAAG	GAGATGAAGATGGACGGCTT	Mm00433121_m1
Otoferlin	NM_001100395	TAAGAACCTGCTTCGGAGC	CAACCCAGCAGAGATGTCAT	Mm00453306_m1
Parvalbumin	NM_013645	TGCAGGATGTCGATGACAGAC	TCAGGCCCACCATCTGGA	*

*custom made assay:
Taqman probe: TCGCCTTCTTGATGTCCTCAGCGCT
Sense primer for real-time PCR: TTTCGCACTTGCTCTGC
Antisense primer for real-time PCR: AATGGACCCCAGCTCATC

Supplementary Table 2: Sequences of external primers and taqman assays used for real-time PCR.

Supplementary Methods:

Animals

Mouse mutants, wild-type littermates as well as C57BL/6 mice were used for experiments. The animals were maintained according to the animal welfare guidelines of the University of Göttingen and the State of Lower Saxony. Animal handling and experiments complied with national animal care guidelines and were approved by the Animal Welfare Office of the state of Lower Saxony.

Cell Physiology

IHCs from the apical coils of freshly dissected organs of Corti or from organotypic cultures prepared from postnatal mice (C57BL/6, lethal-wasting, synaptophluorin knock-in; postnatal day 13 [P13] to 17 [P17]) or SNARE-null animals recovered by Cesarean section at embryonic days 17–19 (synaptobrevin2/3 double knock-out and SNAP-25 knock-out) were patch-clamped at their basolateral side at room or physiological temperature in ruptured-patch or perforated-patch, whole-cell configuration as previously described[8].

The pipette solution for ruptured-patch experiments contained (in mM): 135 Cs-glutamate, 10 tetraethylammonium-Cl (TEA-Cl), 10 Cs-HEPES, 1 $MgCl_2$, 10 4-aminopyridine (4-AP), 2 Mg-ATP, 0.3 Na-GTP, 0.1 fura-2; for toxin-conjugated Alexa, 0.1 mM fura-2 was replaced by 0.1 mM EGTA; for perforated-patch recordings (in mM): 130 Cs-gluconate, 10 TEA-Cl, 10 Cs-HEPES, 1 $MgCl_2$ and 10 4-AP as well as 300 $\mu g \times ml^{-1}$ amphotericin B. The extracellular solution contained (in mM): 105 NaCl, 35 TEA-Cl, 2.8 KCl, 1 $MgCl_2$, 10 Na-HEPES, 1 CsCl and 11.1 D-glucose and 2 or 10 (for knock-out experiments) $CaCl_2$. To control for toxin efficiency, chromaffin cells from mouse adrenal glands were prepared and cultured as previously described[9]. The extracellular solution for chromaffin cells contained (in mM): 105 NaCl, 2.8 KCl, 1 $MgCl_2$, 10 Na-HEPES, 2 $CaCl_2$ and 11.1 D-glucose. All solutions were adjusted to pH 7.2 and had osmolarities between 290 and 310 $mosm \times l^{-1}$. The pipette solution for flash-photolysis contained (in mM): 83 Cs-gluconate, 16 TEA-Cl, 18 Cs-HEPES (pH 7.2), 0.3 mag-fura-2 (Invitrogen, Karlsruhe, Germany), 10 DM-nitrophen (gift of A. Leonov and C. Griesinger, Göttingen), 5 DPTA (1,3-diaminopropan-2-ol-tetraacetic acid) and 10 $CaCl_2$. The extracellular solution for flash-photolysis contained (in mM): 97 NaCl, 35

TEA-Cl, 2.8 KCl, 10 $CaCl_2$, 1 $MgCl_2$, 10 Na-HEPES, 1 CsCl, 11.1 D-glucose (pH 7.2). All chemicals were obtained from Sigma (Munich, Germany), with the exception of amphotericin B (Calbiochem, La Jolla, CA, USA). Neurotoxins (light chain) and trypsin were loaded into cells via the patch pipette. Toxins and trypsin tended to prevent sealing of the patch pipettes to the plasma membrane. Therefore, pipettes were pre-dipped into toxin/enzyme-free solution for 20 to 30 seconds. The concentration of light chain neurotoxins in the pipette solution was 2 μM except for the inactive BoNT/D light chain, where it was 500 nM. The concentration of trypsin was 25.2 μM. IHC Ca^{2+} current integrals were calculated from the total depolarization-evoked inward current, including Ca^{2+} tail currents following P/10 leak subtraction (i.e. from the start of the depolarization step to 1.5 ms after hyperpolarization). Cells that displayed a membrane current exceeding –50 pA at a holding potential of –87 mV were discarded from the analysis. No series resistance (R_s) compensation was applied. Currents were low-pass filtered at 4 kHz and sampled at 10 kHz for capacitance measurements and at 40 kHz for Ca^{2+} current voltage relationships. All voltages were corrected for liquid junction potentials between pipette and bath (calculated: 17 mV). Fura-2 and Alexa were excited at 350/380 nm and 480 nm, respectively, using a monochromator (TILL-photonics, Graefelfing, Germany) and imaged with a CCD camera (IMAGO, TILL-photonics). 8 x 8 pixel binning was used together with long exposure times (50 ms), and emitted light was calculated from background-corrected fluorescence in the IHC area. C_m was measured using the Lindau–Neher technique, implemented in the software-lockin module of Pulse (HEKA Elektronik, Lambrecht, Germany) combined with compensation of pipette and resting cell capacitances by the EPC-9 (HEKA Elektronik) compensation circuitries. A 1 kHz, 70 mV peak-to-peak sinusoidal voltage was applied about the holding potential of –87 mV. ΔC_m was estimated as the difference of the mean C_m over 400 ms after the end of the depolarization (the initial 250 ms were skipped) and the mean prepulse capacitance (400 ms). Data analysis was performed using Igor Pro software (Wave-Metrics, Lake Oswego, OR, USA). Means are expressed ± s.e.m. and compared by Student's unpaired t-test or the Mann-Whitney-U-test as specified. For perforated patch-clamp, mean ΔC_m and Ca^{2+} current estimates present grand averages calculated from the mean estimates of individual IHCs.

Nature Neuroscience: doi:10.1038/nn.2774

Flash photolysis of caged calcium

Flash photolysis was performed as previously described[10] with the following modifications: To obtain step-wise increases in intracellular calcium, DM-NP was uncaged during 100 µs of pulsed laser light using a DPSL-355/1000 UV laser (Rapp OptoElectronic, Hamburg, Germany). The mag-fura-2 was excited with light alternating between 340 and 380 nm using a TILL Photonics system. The amplitudes of individual traces averaged across 200 ms (from 100 to 300 ms after flash trigger) were tested for significant differences.

Plasmid construction

In order to obtain BoNT light chains at high concentration for Alexa488 labeling expression vectors for C-terminally truncated BoNT/C and D light chains were constructed by means of PCR in pQE expression vectors (Qiagen, Hilden). The shortened BoNT/C and D light chains lacked the C-terminal 20 and 10 amino acids, thus ending in Leu-430 and Val-436, respectively. The truncated light chains exhibited a slightly reduced proteolytic activity compared to their corresponding full-length light chain, but strongly increased solubility (data not shown).

Expression, purification and labeling of BoNT light chain

Recombinant BoNT light chains were produced in *E. coli* M15pREP4 during 3 h of induction at 21°C and purified on Ni^{2+}-nitrilotriacetic acid-agarose beads according to the manufacturer's instructions. Purified light chains were dialyzed against 100 mM NaCl, 10 mM HEPES-NaOH, pH 7.2, if destined for Alexa488 labeling. Labeling was conducted using the Alexa fluor®488 protein labeling kit (Invitrogen) according to the manufacturer's protocol. Alexa488-conjugated light chain and unlabeled light chain preparations were dialyzed against 135 mM glutamate, 10 mM HEPES-CsOH, pH 7.2, finally frozen in liquid nitrogen, and kept at –70°C. Protein concentrations were determined following SDS-PAGE analysis and Coomassie blue staining by means of the LAS-3000 imaging system (Fuji Photo Film, Co., Ltd.) and the AIDA 3.51 program using various known concentrations of bovine serum albumin run as standards.

In vitro substrate cleavage assays

SNAP-25 and synaptobrevin-2, were either generated by *in vitro* transcription/translation using the SP6/T7 coupled TNT reticulocyte lysate system (Promega, Mannheim, Germany), and [^{35}S]methionine (37 TBq/mmol, Amersham Pharmacia Biotech, Freiburg, Germany) according to the manufacturer´s instructions or were produced as His6-tagged proteins in *E. coli* M15pREP4. Cleavage assays contained 1 µl of the transcription/translation mixture or a 10 µM concentration of substrate produced in *E. coli* and the specified concentration of BoNT light chain. Reactions were incubated for the indicated time at 37°C in a total volume of 10 µl of toxin assay buffer (150 mM K-glutamate, 10 mM HEPES-KOH, pH 7.2). Reactions were stopped by the addition of an equal volume of double-concentrated sample buffer [120 mM Tris-HCl, pH 6.75, 10% (v/v) β-mercaptoethanol, 4% (w/v) SDS, 20% (w/v) glycerol, 0.014% (w/v) bromphenol blue]. Samples were analyzed by SDS-PAGE. Proteins were visualized by Coomassie blue staining and the LAS-3000 imaging system (Fuji Photo Film, Tokyo, Japan) or, if radiolabeled, by employing a BAS-1500 phosphoimager. Quantification of unlabeled and radiolabeled proteins was done with the Tina 2.09 and the AIDA 3.51 software, respectively.

Single Cell PCR

A single cell PCR approach to detect several different mRNAs in individual cells was performed. Briefly, the cytoplasm of individual IHCs at postnatal days 14-15 was sucked into a patch-pipette containing 8 µl pipette solution (in mM: 150 KCl, 1 $MgCl_2$, 10 HEPES). The total content of the patch-pipette was blown by air pressure into a reaction tube containing buffers for reverse transcription (2.5 µl first strand buffer, 0.6 µl Oligo dT (0.5 µg/µl), 0.5 µl random hexamers (0.2 µg/µl), 0.7 µl dNTPs (10 mM each), 1.4 µl DTT (0.1 M), 0.8 µl RNAseOut and 0.5 µl Superscript II, all chemicals from Invitrogen). cDNA was synthesized and ethanol precipitated. The cDNA of each of the 20 IHCs was used as template for multiplex PCR using “external” primers (see Supplementary Table 2) with 15 standard PCR cycles. Amplification efficiency of the external primers in the multiplex PCR was tested with Sybr green Real-Time PCR in a separate assay using mouse brain cDNA as template. The multiplex PCR served to pre-amplify the amplicons

used for taqman qPCR, which was performed in individual reaction tubes for each target gene and IHC (for assays see Supplementary Table 2). For controls, we sucked external bath solution close to the IHCs into a patch pipette and processed it exactly as the cells. In two out of three bath controls, we detected otoferlin mRNA, however with at least 31-fold lower abundance than in any of the IHCs. All other assays in all bath controls were negative. As positive control, we used a high dilution (1:1000) of mouse brain cDNA (without multiplex PCR).

Immunohistochemistry

Cryosections of cochlea from 2-week-old C57BL/6 mice were prepared as follows: Cochleae were dissected in ice-cold HEPES-Hank's solution, fixed using short perfusion with 4% paraformaldehyde in PBS followed by 1 h incubation in the solution, washed in PBS, cryo-protected by overnight incubation in 25% Sucrose in PBS at 4°C, incubated 2h in Tissue Tek (Shandon Cryomatrix, Thermo Scientific, UK) on a rocker, and frozen over liquid nitrogen. 14 µm cryosections were stored at –80°C. The frozen sections were thawed and dried at room temperature, rehydrated 25 min in PBS, followed by incubation for 1 h in goat serum dilution buffer (16% normal goat serum, 450 mM NaCl, 0.3% Triton X-100, 20 mM phosphate buffer, pH 7.4); primary antibodies were applied overnight at 4°C. Secondary Alexa-labeled antibodies were applied for 1 h at room temperature. The images were acquired using Leica TCS SP2 or SP5 laser scanning confocal microscopes.

References

1. Miesenböck, G., De Angelis, D.A. & Rothman, J.E. Visualizing secretion and synaptic transmission with pH-sensitive green fluorescent proteins. *Nature* **394**, 192-195 (1998).
2. Safieddine, S. & Wenthold, R.J. SNARE complex at the ribbon synapses of cochlear hair cells: analysis of synaptic vesicle- and synaptic membrane-associated proteins. *European Journal of Neuroscience* **11**, 803-812 (1999).
3. Lenzi, D., Runyeon, J.W., Crum, J., Ellisman, M.H. & Roberts, W.M. Synaptic Vesicle Populations in Saccular Hair Cells Reconstructed by Electron Tomography. *J. Neurosci.* **19**, 119-132 (1999).
4. Xu, T., Binz, T., Niemann, H. & Neher, E. Multiple kinetic components of exocytosis distinguished by neurotoxin sensitivity. *Nat. Neurosci* **1**, 192-200 (1998).

5. Pusch, M. & Neher, E. Rates of diffusional exchange between small cells and a measuring patch pipette. *Pflugers Arch.* **411**, 204-211 (1988).
6. Plattner, H., Artalejo, A.R. & Neher, E. Ultrastructural Organization of Bovine Chromaffin Cell Cortex—Analysis by Cryofixation and Morphometry of Aspects Pertinent to Exocytosis. *The Journal of Cell Biology* **139**, 1709 -1717 (1997).
7. Takamori, S. et al. Molecular anatomy of a trafficking organelle. *Cell* **127**, 831-846 (2006).
8. Moser, T. & Beutner, D. Kinetics of exocytosis and endocytosis at the cochlear inner hair cell afferent synapse of the mouse. *Proceedings of the National Academy of Sciences of the United States of America* **97**, 883-888 (2000).
9. Sorensen, J.B. et al. Sequential N- to C-terminal SNARE complex assembly drives priming and fusion of secretory vesicles. *EMBO J* **25**, 955-966 (2006).
10. Roux, I. et al. Otoferlin, Defective in a Human Deafness Form, Is Essential for Exocytosis at the Auditory Ribbon Synapse. *Cell* **127**, 277-289 (2006).